The influence of cutting parameters on the defect structure of subsurface in orthogonal cutting of titanium alloy

Jinxuan Bai[1*], Qingshun Bai[1*], Zhen Tong[2], Guoda Chen[3]

1 School of Mechanical and Electrical Engineering, Harbin Institute of Technology, Harbin 150001, China

2 Centre for Precision Technologies, University of Huddersfield, Huddersfield HD1 3DH, UK

3 Key Laboratory of E & M, Ministry of Education & Zhejiang Province, Zhejiang University of Technology, Hangzhou 310032, PR China

**Corresponding author:* jinxuanbai@hit.edu.cn; qshbai@hit.edu.cn

Abstract: Subsurface microstructure alteration has been a major concern to implement micro-machining of titanium alloy in high-tech industry. To quantitatively promulgate the underlying mechanisms of this alteration, a discrete dislocation dynamics-based model is proposed and used to simulate the subsurface defects and their evolution under different cutting conditions. The model considers the subsurface dislocation configuration and inner stress distribution during the orthogonal cutting of titanium alloy. The results show that subsurface defect structure consists of plenty of dislocation dipoles, twining dislocation bands and refined grains after cutting. In primary shear zone, two different characteristics of subsurface damage layers can be found, near-surface damage layer and deep-surface damage layer, which have different structural natures and distribution features. Moreover, it is found that high cutting speed and small depth of cut can suppress the formation and propagation of subsurface defects. Powerful inner stress state would promote the distortion of lattice and result in micro-crack within subsurface matrix. The simulation results have been compared with experimental findings on machined surface and subsurface of similar materials, and strong similarities were revealed and discussed.

Keywords: titanium alloy; subsurface defect structure; inner stress; dislocation dynamics

1 Introduction

Titanium and its alloys have become key supporting materials in biomedical and aerospace industry due to their excellent comprehensive mechanical properties and the improvements made on machining these alloys [1, 2]. According to Ulutan and Tan [3, 4], a typical characteristic of titanium alloy machined surface consists mainly of three parts: surface white layer, subsurface plastic deformation zone and bulk material. In previous studies, surface white layer states for processed components have attracted substantial efforts in academic and application field [5, 6]. However, with the increasing demands for machined precision and surface quality in micro-machining process, it is important to recognize that the mechanical properties and lifetime of workpiece are determined by no means only the shape or precision of machined surface, the characteristics of subsurface microstructure may dominate the component's service performance and reliability, as well [7]. Specially, the change of subsurface microstructure and the release of residual stress caused by powerful shearing action would result in inherent deformation and form subsurface damage (SSD) layer underneath surface. The presence of damage layer can inevitably deteriorate the structural and functional performance of finished components, such as weakening machined surface strength, affecting the application durability and secular stability of end parts. In this context, the evaluation of subsurface microstructure alteration and defects distribution would exhibit a critical role in optimizing machining parameters and processing efficiency.

Research showed that the most of major threats to finished surface were derived from workpiece subsurface microstructure evolution during micro-cutting process [8]. Therefore, to further illuminate the formation and influence mechanisms of subsurface defects, lots of experimental and theoretical studies have been carried out.

Ginting et al. [9] focused on processed subsurface quality in dry cutting titanium alloy. Experimental observations concluded that the subsurface area took place remarkable plastic deformation and microstructure alteration. Thomas et al. [10] argued that the microstructural subsurface damages were detected in the form of intense slip bands after micro-milling of titanium alloy. Such damages can degrade in-service properties of component because of a reduction in fatigue crack initiation resistance. Kwong et al. [11] indicated that the subsurface damage layer may also result in micro-crack in bulk material. In addition, during micro-cutting process, it is known that the subsurface microstructure alteration is mainly influenced by a series of intrinsic and extrinsic parameters such as, processing parameters, tool structure and material properties. Jin et al. [12] stipulated that machining parameters played a vital role in the formation of subsurface damage layer in orthogonal milling of FGH95 superalloy. Lv et al. [13] proposed a non-traditional technology to measure the thickness and distribution of subsurface damage layer during rotary ultrasonic machining of glass BK7 process. Results showed that the subsurface damage depth generated in cutting process was directly proportional to the increased cutting depth and feed speed of cutter tool. To et al. [14] presented experiments to reveal the influence of microstructural changes under various axial depths of cut on machined surface textures during micro-turning process. They found that the microstructure evolution simultaneously ensued and enhanced the uncertainty of surface topography relating to workpiece swelling, recovery and surface finish. Furthermore, after micro-cutting process, the defect structure of subsurface tends to store lots of micro-inner stress [15]. Comparing with the residual stress, it always presents greater potential risks in terms of crack initiation, evolution and fatigue failure within end components [16]. However, although foregoing experimental data can reflect a certain of subsurface characteristics, this special worth pointing out that no predictive, experimental or numerical work has ever been presented to quantitatively track the formation and propagation mechanism of workpiece subsurface damages.

Recently, orthogonal cutting simulation has been exploited as a means for investigating the surface and subsurface microstructure alteration for various materials [17]. Shin et al. [18] developed a finite element analysis framework to predict the machined chip and surface grain refinement process. However, a key limitation of their model is that the constitutive equation depends only on dislocation-based model $d=K\rho^{0.5}$, where K is material constant, d and ρ are grain size and dislocation density, respectively. It indicates that the grain would take place continuous changes if the external load is enough to cause a net increase of total dislocation density. Not only that, the multiplication and evolution of dislocation in previous physically based modelling approaches were simple predicted as a function of strain, which cannot precisely factor in the interaction among dislocations, grain boundaries and crystal defects [19]. According to molecular dynamics (MD) method, Wang et al. [20] studied the stress-induced formation mechanism of subsurface stacking fault tetrahedra during nano-cutting crystalline copper process. Li et al. [21] analyzed the effect of various tool radii, crystal orientations and machining angles on subsurface deformation layer in nanoscale grinding. However, due to the limitation of analytical scale, the simple materials models and extreme cutting parameters resulted that atomistic computer simulation not only cannot trace numerous subsurface defects interaction in complex cutting conditions, but would suppress the nucleation of subsurface dislocation. Particularly, as a typical mesoscale simulation way, discrete dislocation dynamics (DDD) could offer better scalability to conduct more intricate problems relative to MD way with larger time scale and space scale. Also, the DDD analytical method would provide better angle of vision into some aspects of material mechanical behaviors heretofore not uncovered by using continuum approaches, such as the transmutation of dislocation structure. Shishvan et al. [22, 23] showed that simpler two-dimensional DDD study is more successful in revealing microstructure evolution and plastic mechanism rather than three-dimensional simulation. Tarleton et al. [24] revealed the micro-cantilever bending of hexagonal close-packed structure crystals for plane strain prismatic slip. Their study showed that the inhomogeneous and highly localized internal damages distribution would influence surface strengthening. Especially, on the basic of dislocation dynamics theory, the authors [15]

developed a new trans-scale cutting framework to reveal the refinement process of surface grain structure in micro-machining Ti-6Al-4V. Results indicated that the predications of simulations were commensurate within experimental scope. Thus, DDD can provide an effective way to reveal the subsurface microstructural changes and inner stress distribution during micro-cutting process.

In present work, a series of discrete dislocation dynamics-based simulations were performed to qualitatively and quantitatively assert the distribution of subsurface defect structure and its evolution during the orthogonal cutting process of titanium alloy under different cutting conditions, which for the first time considers both grain refinement and large-scale interaction among defects. Moreover, the influence of various processing parameters on subsurface microstructure alteration and inner stress field distribution were discussed. To this end, the paper is consisted of the following key parts. Section 2 introduces the subsurface damage mechanism of titanium alloy. Section 3 provides a brief description about the trans-scale coupling algorithm. Section 4 gives detailed simulation results and discussion. Section 5 summarizes the manuscript with some main conclusions.

2 Subsurface damage of titanium alloy in cutting process

Studies on titanium alloy have showed that a damage layer can be found in the immediate subsurface deformation zone of the workpiece, and as the increment of tool wear, plastic deformation and subsequently the thickness of damage layer increased due to subsurface microstructural alteration [5, 25]. Moreover, the depth of damage layer beneath the finished surface was observed to change as the evolution of cutting depth and feed rate, and the increase of cutting speed from low level to high level would produce more serious grain refinement in subsurface [9]. However, some conflicting experimental results about the average depth of subsurface damage layer from electron microscopy and electron backscattered diffraction (EBSD) were also found during micro-cutting titanium alloy process, which have implication for the effectiveness of current surface integrity research to determine the features of subsurface deformation for finished titanium alloy [26].

As the workpiece material investigated in present study, Ti-6Al-4V is composed of equiaxed alpha grains and a small quantity of intergranular beta phase [27]. According to the EBSD results, Fig. 1 (a) and (b) indicated the influence of subsurface plastic strain imparted on Ti–6Al–4V and Ti-834 during milling process. It is found that the subsurface damage layer is principally accommodated by dislocation evolution and slip bands within alpha phase grains [10]. In particular, on the basic of Liu et al. [28], the effect of beta-titanium on subsurface plastic deformation can be ignored in cutting simulation process due to the low volume fraction of beta phase, which is not more than 8%. Thus, it is reasonable to assume that only alpha grains were considered in present study, and indicating that the subsurface zone was composed of hexagonal close-packed (HCP) structural crystals. Moreover, it is noteworthy that the low stacking fault energy for HCP crystal means that the transition of subsurface defect structure largely focusses on dislocation evolution rather than stacking faults [15, 24].

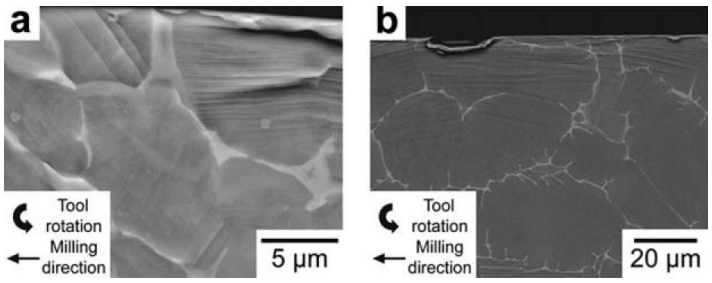

Fig. 1 Plastic deformation in the form of intense slip bands (a) Ti–6Al–4V and (b) Ti-834 [10].

3 Dislocation dynamics-based simulation framework for micro-cutting

3.1 Method of dislocation dynamics

In this work, a trans-scale coupling framework was performed by embedding discrete dislocation dynamics algorithm into a finite-element package via Python and Matlab scripting. This framework incorporated two characteristic scales, nanometer scale and continuum scale. For the former one, short-range phenomena, containing dislocation motion, junction, immobilization, interaction and spatial rearrangement, were calculated by DDD simulation. In continuum scale, finite element method (FEM) solver was used for long-range solution of elastic driving stress of dislocations during micro-cutting process. As a typical line defect, the movement of dislocation is firmly controlled by Peach-Koehler (*P-K*) force [29], which can be written as

$$f_g^{(I)} = \left(\sigma + \sum_{J \neq I} \sigma_{ij}^{(J)}\right) b_j^{(I)} m_i \quad , \tag{1a}$$

$$f_c^{(I)} = -\left(\sigma + \sum_{J \neq I} \sigma_{ij}^{(J)}\right) b_j^{(I)} s_i \quad . \tag{1b}$$

Where σ_{ij} denotes the internal stress field caused by other defects, σ denotes the external stress state on the glide plane, $f_g^{(I)}$ denotes the slip force, $f_c^{(I)}$ denotes the climb force, $b_j^{(I)}$ denotes the Burger's vector of dislocation *I*, and $\{m_i, s_i\}$ are unit normal and unit vector in the slip direction, respectively.

In DDD algorithm, the series of dislocation behaviors, such as dislocation nucleation and close encounters, must be governed by particular principles [30]. A mass of analogous Frank-Read (*F-R*) sources are randomly distributed throughout slip system, which possess intrinsic nucleation strength and nucleation time. A new nucleation event contains a pair of dislocations can be generated in the form of dislocation dipoles. Similarly, the location of pre-existing obstacles is also on the basis of stochastic distribution on the glide planes. Specially, in order to reveal sufficiently the evolution process of subsurface microstructure, a series of improvement constitutive rules are established to incorporate three-dimensional dislocation features into plane simulation, such as dislocation cross slip and dynamic junction formation, which may also act as potential points for *F-R* sources [31]. In addition, the dislocation is allowed to move out of original slip plane when its climb distance is larger than the magnitude of Burgers vector [32, 33]. The mobile dislocations on intersectional slip planes would have locks if they are close enough together, which could form the new dislocation obstacles and impede subsequent dislocations. Moreover, opposite sign dislocations will be spontaneous annihilation when they come within a cut-off distance of 6*b*.

3.2 Modeling details

The trans-scale simulation model used in this paper was shown in Fig. 2. Linear quadrilateral CPE4R planar strain element with enhanced hourglass control was chosen into temperature-displacement coupling analysis. In order to optimize the contact control during micro-cutting process, a multi-part FEM model was typically modeled [34]. The dimensions of workpiece material were 30 μm×12 μm. In this model, Part1 is uncut chip thickness, Part 2 is tool-tip surface contact zone, Part 3 is material support zone and Part 4 is insert active cutting tool. In addition, diamond tool was developed with normal rake angle 15 °and flank angle 6 °. The enter angle and inclination angle were 90 °and 0 °, respectively. The radius of the cutting edge was 0.25 μm. Then various cutting depths and cutting speeds were conducted to reveal the evolution mechanism of subsurface defects.

Abaqus with explicit solver was adopted to improve the physical comprehension of subsurface damage layer during orthogonal cutting titanium alloy. To capture the distribution of external applied stress of finite element (FE) nodes in subsurface, fully coupled thermos-mechanical analysis was employed within time step 0.5 ns. The boundary value problem of subsurface support zone was solved in FE module, which treated a mass of individual

dislocations as the carriers of persistent subsurface plastic deformation [15]. Further, the image stress σ^{NOD} at element node was calculated by subtracting the intrinsic stress produced by surrounding dislocations. Then, elastic driving stress field of dislocation *I* could be obtained by linear interpolation algorithm. Finally, the computational results of each increment were constantly input to DDD module, where the dislocation nucleation, accumulation, recovery and annihilation were tracked [35]. As shown in Fig. 2 (a), a two-dimensional representative HCP cell model was built to explore the dislocation propagation rules in support area. According to previous study [24, 26], discrete dislocation of titanium alloy moves in <1 1 -2 0> slip direction and on {1 0 -1 0} slip plane. Therefore, reference slip directions {0˚, 60˚, 120˚} on the base of the x-axis were shown in Fig. 1 (a). In addition, some detailed constants related to present study were listed in Table 1.

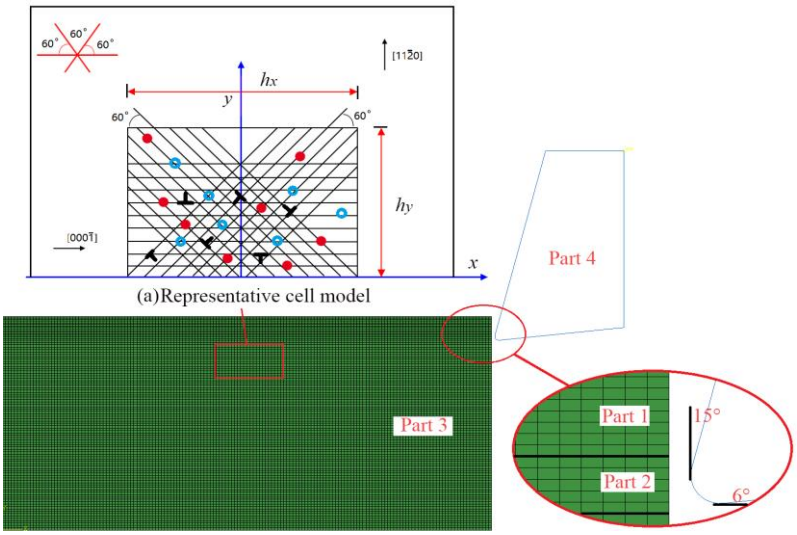

Fig. 2 Trans-scale simulation model. (a) representative cell model. The mesoscale material model consists of dislocation sources (solid circle), obstacle sources (open circle), pre-existing dislocations, slip system, grain boundary and so on.

Table. 1 Material constants of titanium alloy.

Parameter	Value
Vacancy self-diffusion energy (ΔE_{sd})	2.509 eV
Pre-exponential diffusion constant (D_0)	0.015 cm^2/s
Gliding drag coefficient (B_g)	1.4×10^{-4} Pa s
P-N force (f_0)	0.02 MPa
Nucleation stress (τ_{nuc})	0.8 GPa
pre-existing dislocation density	6.25×10^{12} m^{-2}
dislocation sources density	4.2×10^{13} m^{-2}
obstacle sources density	2.1×10^{13} m^{-2}

4 Results and discussion

4.1 Dislocation nucleation and the structural transformation of subsurface defect

Subsurface states and their modifications induced by the complex interaction between cutting force and residual force play a vital role in micro-machining process. It leads to lots of fascinating microstructure consequences. To discover above features, a series of snapshots of FEM-DDD observations were shown as Fig. 3, which demonstrated the generation and reaction process of subsurface damages. Meanwhile, local representative zone was adopted to further reveal the detailed characteristics of subsurface microstructure changes. During simulations, a mass of dislocations nucleated from static random F-R sources would arrange themselves into specific

configurations to the accommodation of matrix deformation. It can be seen that these defects either formed dislocation dipoles on parallel slip planes, dislocation junctions and locks on crossed slip planes, or piled-up against grain boundaries.

Acting under external stress, great quantities of dislocations were generated and extended in Fig. 3 (a). Accompanying with the accumulation and release of cutting energy, the distribution of subsurface damage layer continuously evolves with the increasing of cutting length. Dislocations emitted in vertical direction downward promote the formation of dipoles immediately below cutting tool. The interactions between feed force and thrust force give a boost to various evolution behaviors of subsurface defects, including dislocation processes of nucleation, motion, annihilation and so on. Above results cause the interaction among dislocations and other possible defects and facilitate the build-up of complicated dislocation networks, which are greatly favorable for generation and storage of internal stress in the workpiece subsurface.

As the cutting distance reached 5 μm, obvious dislocation lines which were nearly $\pm 45°$ with the slip direction were formed in the representative zone, as shown in Fig. 3 (b). Meanwhile, the shearing action of cutting tool further promoted the quantity mushrooming of edge and screw dislocations. Simulation results indicate that the length of subsurface damage layer indeed increases along tool path, but its depth then basically remains stable. The underlying reasons is that the subsurface damage layer microstructure possesses a series of invariable formation mechanism during steady cutting process. Specially, two types of subsurface defect structures can be identified, near-surface damage layer (from upper surface to near 2 μm depth subsurface) and deep-surface damage layer (from the bottom of near-surface damage layer to deeper substrate) respectively, which has totally different structural natures and defects distribution characteristics. It is noteworthy that the prediction of multilayer damage shows a satisfied agreement with the previous experimental phenomena, which suggested that the subsurface damage resulting from micro-cutting can permeate deeper into base material than previous reported [10]. In particular, since the near-surface damage layer mainly occurs in a very narrow region of subsurface, it easily forms subsurface work-hardening due to densely tangled among dislocations. Instead, the deep-surface zone may contain little free dislocations and localization obstacles under certain conditions, hence the slight dislocation slip without constraint would produce strain softening in the fundamental part. Above obtained result coincides well with Guo et al. [36], which argued that the hardness data measured in deep subsurface is slightly less than the bulk material in some conditions. In addition, with the increase of cutting length, lots of dislocations were hampered by vacancy cluster defects and locks, which lead to the formation of subsurface hardening layer and restrain plastic deformation. Particularly, Fig. 3 showed that not only near-surface damage layer but deep-surface zone formed unique dislocation bands at the moment of tool cut-in, which uninterruptedly migrated under the squeeze action of the cutting tool. Its reason is that the instantaneous impulsion of cutting tool causes the continuous dislocation emission of grain boundary in deeper subsurface zone.

With the proceeding of machining, dislocations were condensed into tangles. Subsurface matrix gradually generated several persistent slip bands (PSBs), as shown in Fig. 3 (c). The PSBs as crystal structure can form barriers to impede the sequent dislocation motion and then intensify the pile-up hardening effect in subsurface. At the same time, serious external action would further facilitate the elongation and reorientation of PSBs in shear direction. Since dense slip bands possess higher dislocation density than the rest of zone, the distribution of subsurface defects tends to be inhomogeneous, causing significant strain concentration. It is worth mentioning that the squash and stretch effect among PSBs and free-dislocation crystal structures may result in micro-crack initiation, propagation and coalescence. Above simulations are consistent with previous experiment where the principle mechanism for fracture crack initiation is the interaction between slip bands with subsurface grain boundaries or specimen surface [9]. After cutting, the influence of external stress field on deformation zone weakens sharply, but the severe asymmetry of internal stress distribution powerfully promotes succeeding defect

structural evolution. At this stage, dynamic recovery is the main process in forming stable subsurface structure, in which dislocations produced entanglement structure at near-surface zone in Fig. 3 (d). It not only dominates dislocation evolution on particular slip planes but gives rise to subsurface grain refinement, because the migration of dislocations induces enormous vacancy migration energy in subsurface damage layer, then the unbalance of lattice energy transforms original crystal into independent subgrain until refined grain boundaries are constructed.

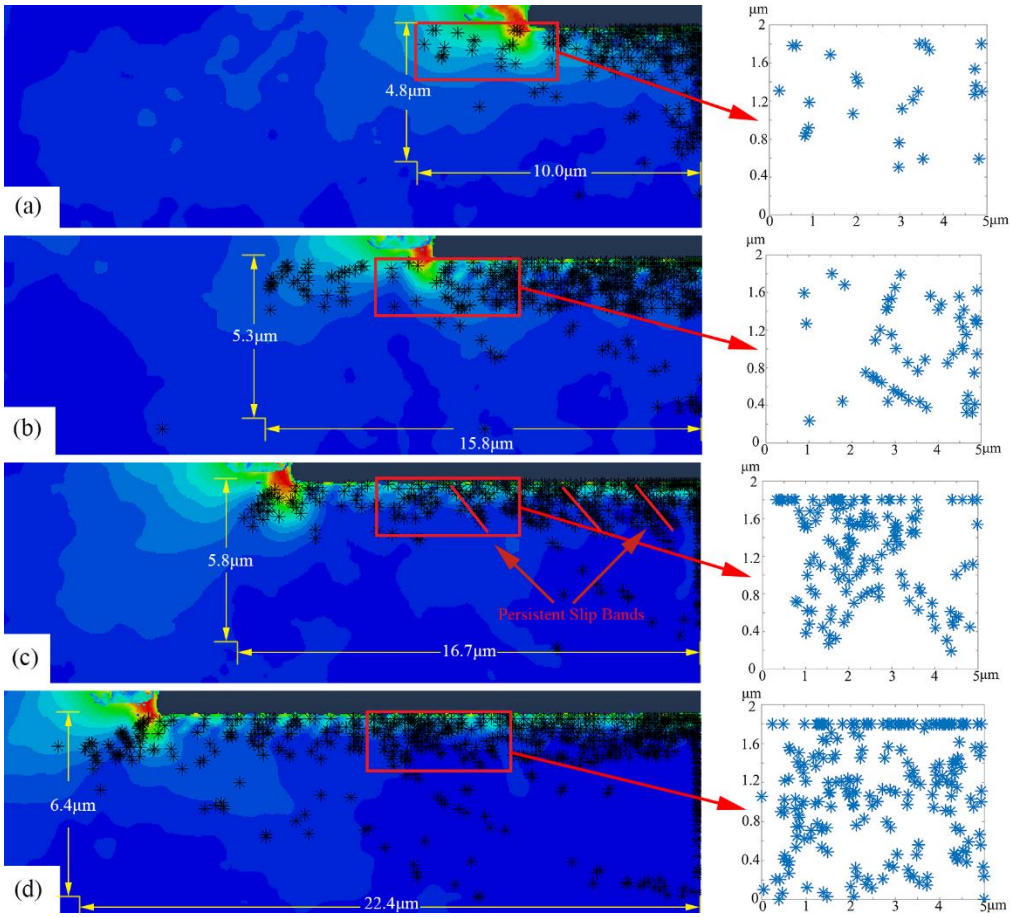

Fig. 3 Dislocation distribution and local dislocation crystal structure against the cutting distance (cutting speed 10 m/s and cutting depth 0.5 μm). (a) cutting distance 5 μm; (b) cutting distance 10 μm; (c) cutting distance 15 μm; (d) cutting distance 20 μm.

4.2 Influence of cutting depth on subsurface defect structure

Cutting parameter plays an important role in the formation of subsurface damage layer by influencing the propagation and retention of dislocations. To clearly illuminate its variation tendency, DD snapshots were specially extracted. According to various cutting depth classifications, cutting depths of 0.5 μm, 1 μm, 2 μm, 3 μm were used for studying subsurface structure changes, while the other machining parameters kept exactly the same, i.e. the cutting speed was 10 m/s. Fig. 4 (a-d) presented selected subsurface morphologies with various cutting depths when the cutting distance was 2.5 μm. As described in the previous section, two distinct subsurface deformation areas of near-surface damage layer and deep-surface damage layer, each characterized by different distribution and array features, were found to constitute and keep subsurface deformation filed. From Fig. 4, we can get that varying cutting depths could lead to entirely different subsurface organizational structures. At small cutting depth in Fig. 4 (a), dislocations primarily focused on near-surface zone, and the slipping and climbing behavior of dislocations made great contribution to the accommodation of microstructure deformation. Subsequently, upon undergoing further increase of cutting depth, the near-surface damage layer consisted of a certain amount of piled-up dislocations and refined grain organizations in Fig. 4 (b). Moreover, it can be seen that larger cutting

depth would activate dislocation nucleation and motion deeper down in subsurface interior. This phenomenon can be explained as that increasing cutting depth conducts a higher impact loading exerted on workpiece, and a larger deviatoric stress provokes in the interior material, hereby increasing the thickness of subsurface damage layer in consequence. On the other hand, as the interaction of impact and friction between tool and workpiece, subsurface damage layer gathers dislocations and forms dense shearing bands, as shown in Fig. 4 (c-d). Specially, when the cutting depth is larger than 2 μm, it is found that the deep-surface dislocations tend to form a larger number of choroid dislocation bands, which slip forwards along glide system with an approximation angle of 30 ° and 60 ° to cutting direction. With the increase of axial depth of cut, they gradually became wider and longer. Particularly, in comparison to subsurface damages in near-surface zone, the accumulation and propagation of dislocations in deep-surface damage layer may result in more serious distortion deformation and stress concentration, which has been studied in more detail later in this work.

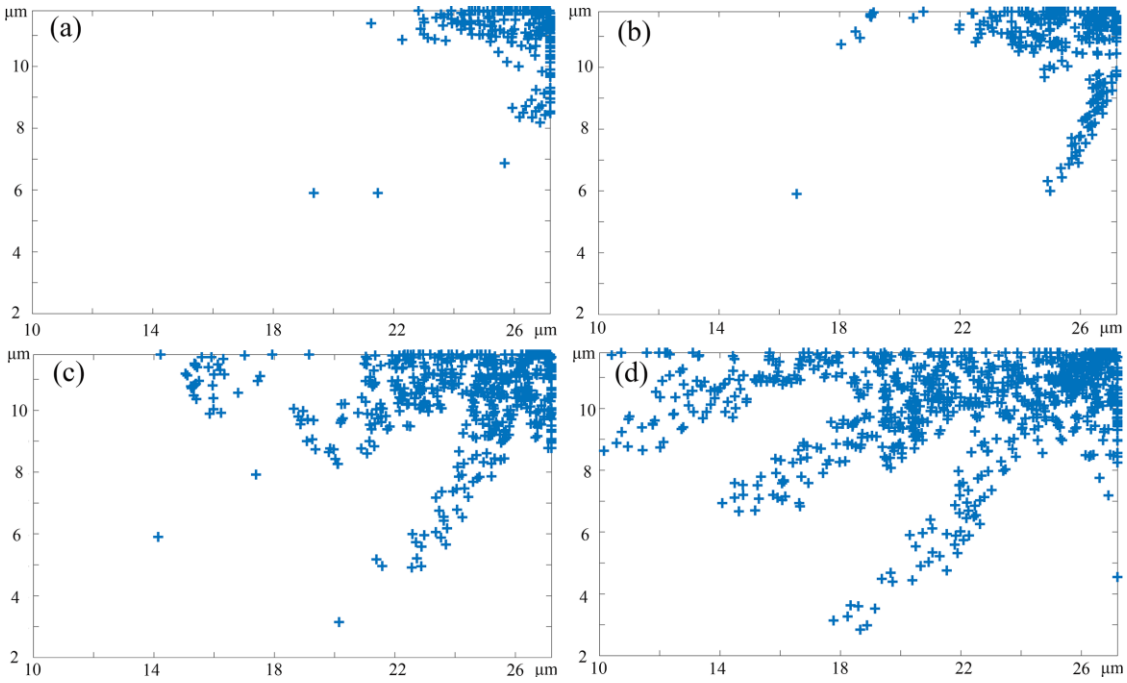

Fig. 4 Subsurface morphology under different depth of cut (a) 0.5 μm, (b) 1 μm, (c) 2 μm, (d) 3 μm. (cutting speed = 10m/s; cutting distance = 2.5 μm)

For subsurface deformation zone, different sorts of evolution processes of damages with the increase of cutting distance were shown in Fig. 5. In the initial stage of micro-cutting process, cut-in impulse forces results that subsurface pre-existing dislocations usually fail to make timely structural adjustments. Therefore, majority F-R sources of titanium alloy have to take place local dislocation multiplication to relieve external stresses. It led to the increasing of dislocations in quantity, as shown in Fig. 5 (a). Based on above analysis, decreasing cutting depth tends to produce relative small hydrostatic pressure in subsurface and indicate less demand for dislocation proliferation so that the number of subsurface dislocations changed slightly when the axial depth of cut is less than 1 μm. Since dislocations are continuous annihilation and removed from simulation area in micro-cutting process, the dislocation quantity kept stability essentially when the cutting length is greater than 25μm. Moreover, the rapid expansion of dislocation density and quantity also boosted the odds of dislocation accumulation nearby cross slip dislocations, junctions, grain and subgrain boundaries, which would govern the exhaustion hardening effect for subsurface damage layer, as shown in Fig. 5 (b) and (c). Additionally, the axial depth of cut had a serious impact on the internal organizational structure of deep-surface damage layer, thus the defects number and their proportion both sharply jumped when the cutting depth was above 2 μm in Fig. 5 (d) and (e). In particular, obstacles and

impurities in near-surface layer would impose restrictions on the locomotivity of individual dislocation, which causes the starvation effect and aggravates the expansion of subsurface damage layer. Therefore, as seen in Fig. 5 (f), SSD depth curves basically kept unchanged in early stage, then presenting a rising trend until reaching the bottom of simulation model.

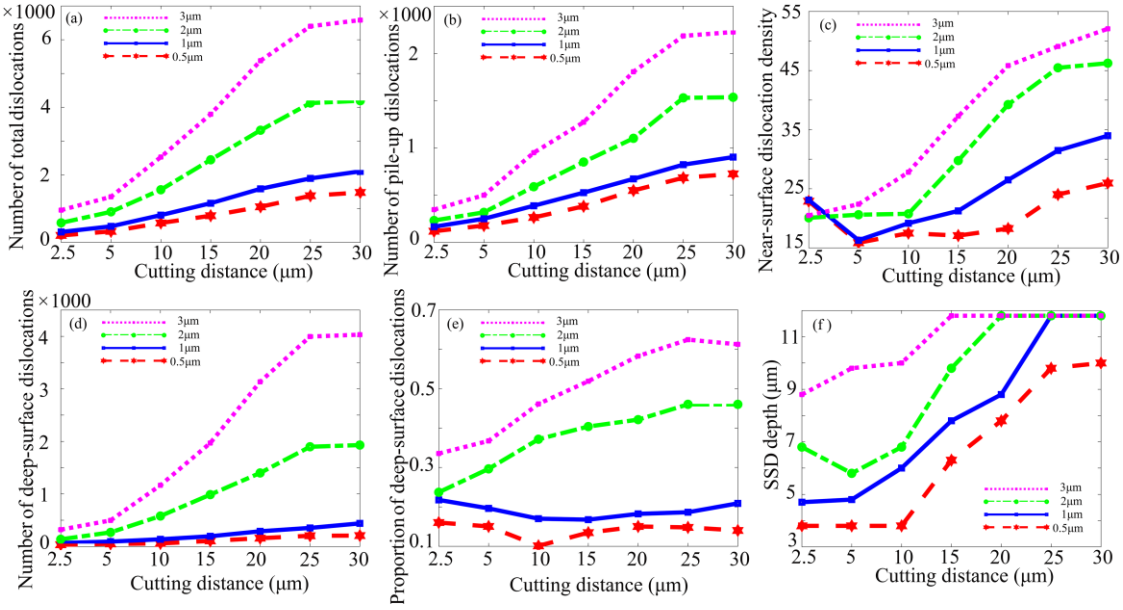

Fig. 5 Evolution of different types of subsurface damages under various cutting depths. (a) number of subsurface dislocations; (b) number of pile-up dislocations; (c) change of near-surface dislocation density; (d) number of deep-surface dislocations; (e) proportion of deep-surface dislocation; (f) change of subsurface damage layer depth.

4.3 Influence of cutting speed on subsurface defect structure

To reveal the influence of cutting speed on subsurface damages structure, several simulation models with various velocities set from 10 m/s to 40 m/s, sharing same depth of cut 1 μm, were developed. The microstructure of machined subsurface shown in Fig. 6 was adopted to quantitatively illustrate the evolution mechanism of inner defects, in which the cutting length was 20 μm. The observations enable us to conclude that machined subsurface presented various characteristics of plastic feature and microstructure alteration from top to bottom. Comparing with different Figures, increasing cutting speed restrained the generation of subsurface defect structure. Actually, the improvement of cutting speed directly raises the temperature in machined surface and subsurface region, which can significantly improve the diffusion constant of the partial dislocation of titanium alloy and enhance the ability of dislocation climb. Since the climbing process helps blocked dislocations jump out of intrinsic slip planes to bypass the local impurity particles and locks, the quantity of immobile defects came down dramatically in Fig. 6 (a-c). But once the cutting speed exceeded specific level, the dislocations facilitated by climb behavior would be more liable to be hindered by impenetrability dislocation bands and grain boundaries. Subsequently, above piled-up phenomena result in the inhomogeneous distribution of subsurface damages and further promote continuous dynamic refinement within grain and subgrain in near-surface damage layer. Furthermore, since the compatible plastic deformation always occurs in refined grain [37], the workpiece subsurface tends to undergo further microstructure alteration without any contribution from dislocation evolution in deep-surface zone, which can hinder the damages from propagating into interior substrate and improve workpiece quality. As a result, when cutting speed reached 40 m/s, discrete dislocations were hardly multiplied in deep-surface damage layer, hence the thickness of subsurface damage layer drops rapidly in Fig. 6 (d).

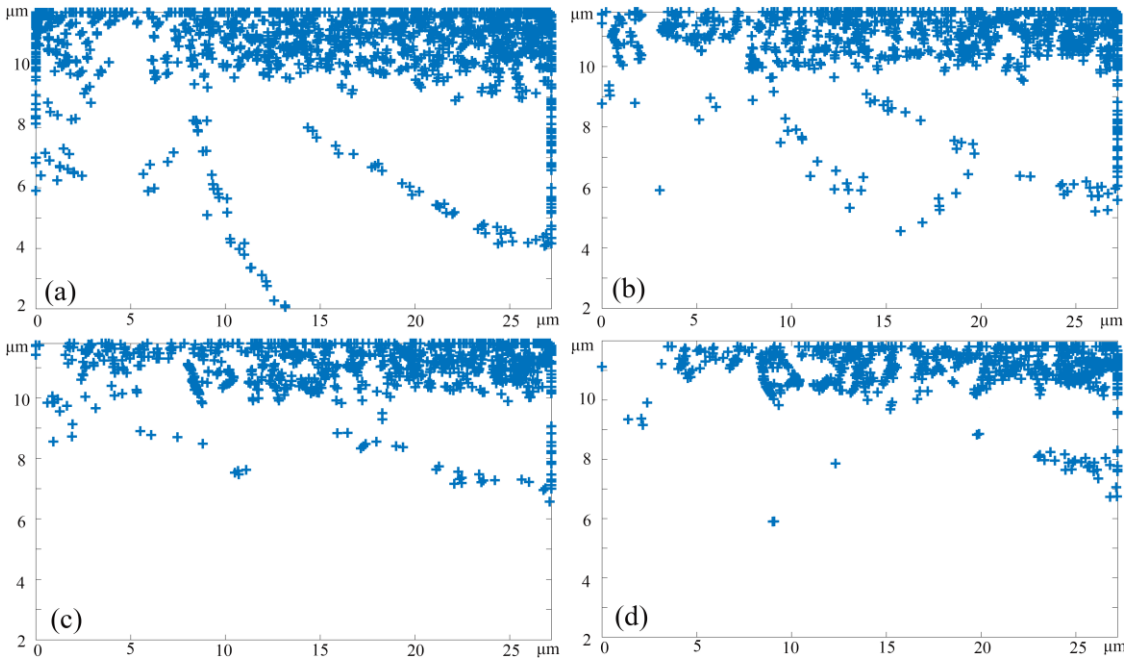

Fig. 6 Subsurface morphology under different cutting speeds (a) 10 m/s, (b) 20 m/s, (c) 30 m/s, (d) 40 m/s. (cutting depth = 1μm; cutting distance = 20 μm)

Fig. 7 indicated different types of curves as a function of cutting speed, where Fig. 7 (a-b) presented the variation of total dislocations and pile-up dislocations, Fig. 7 (c) showed the evolution law of dislocation density in near-surface zone, Fig. 7 (d-e) revealed the number of deep-surface defects and their proportion variations with the cutting distance, and Fig. 7 (f) showed the changes of SSD layer depth in micro-cutting process. With machined surface being formed, the subsurface substrate undergone elastic deformation at first, then shearing visa dislocation movement and grain evolution. From Fig. 7 (a) and (b), the samples with low cutting velocities usually contained greater proportion of impeded dislocations due to lower diffusion coefficient. Therefore, bulk material has to maintain dislocation nucleation to inhibit the formation of subsurface micro-crack caused by partial hardening in the near-surface damage layer. What's more, the amplitude of dislocation number curve increased gradually when the removal velocity arrived at 10 m/s, which was much higher than that for others conditions. Moreover, since back stress caused by obstacle particles always makes it difficult to reactivate *F-R* sources from where dislocations originated, the dislocation density in near-surface zone would display a feature of temporary descending until the occurrence of secondary nucleation on neighboring glide planes, as shown in Fig. 7 (c). As cutting action goes on, the lasting consumption of pre-existing nucleation sources of near-surface deformation zone promotes the initiation and propagation of line defects in deep-surface damage layer when the cutting speed is sufficiently low. Meanwhile, fluctuating thermal stress also leads to a miniature dislocation emission effect from grain boundaries to subsurface internal. Particularly, although grain refinement can decompose external pressure according to previous research, the narrow lattice structure would suppress the generation of dislocation lines and bands if refined grain size fits within submicron scale [15]. In summary, when the cutting speed was larger than 20 m/s, the curve slopes of deep-surface defects quantity and proportion both increased in latter period in Fig. 7 (d-e). As shown in Fig. 7 (f), the increased cutting speed supported the reduction of subsurface damage layer depth, which is opposed by the increase of the cutting depth. Since high material removal rate (MRR) can be obtained by increasing the cutting depth and cutting speed, taking into account the influences of process parameters on SSD and MRR, high cutting efficiency will be obtained while maintaining the subsurface quality.

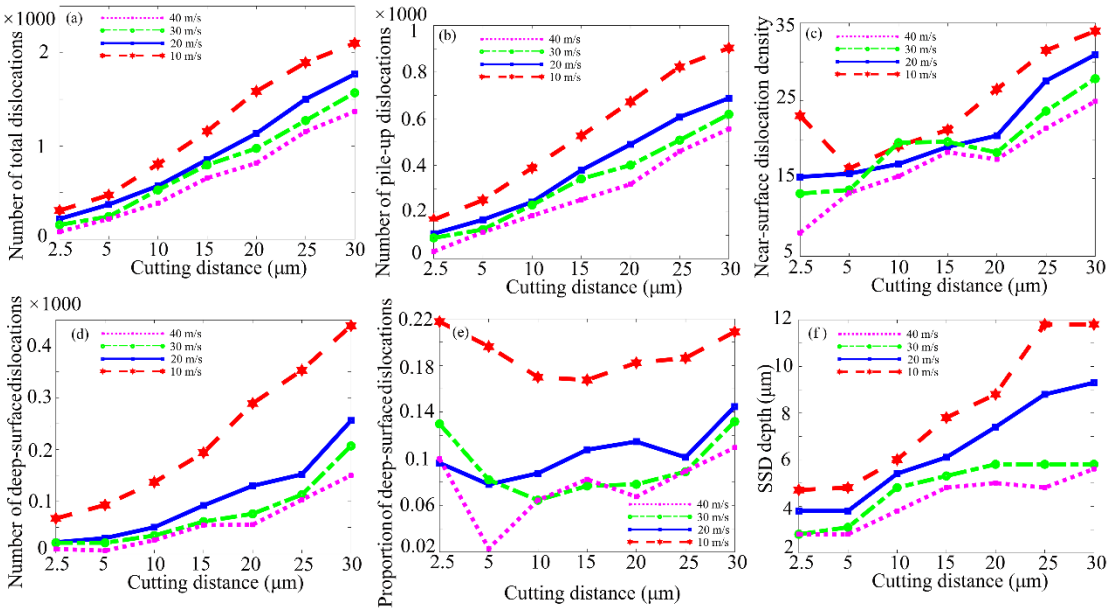

Fig. 7 Evolution of different types of damages in subsurface under various cutting speed. (a) number of subsurface dislocations; (b) number of pile-up dislocations; (c) change of near-surface dislocation density; (d) number of deep-surface dislocations; (e) proportion of deep-surface dislocation; (f) change of subsurface damage layer depth.

4.4 Influence of cutting parameters on subsurface inner stress distribution

Above results indicate that the subsurface microstructure forming process is mainly governed by the strong localization of dislocation evolution and dynamic balance of tool-workpiece contact region. With the penetration of outer tool, external kinetic energy is constantly transmitted into matrix and converted to internal energy via storing in subsurface defects. Once particular threshold has been exceeded, dislocations would be re-arranged into lower energy structure. At last, most of discrete dislocations form a stable self-balanced system within sufficient time durations, which directly results in the forming of subsurface inner stress-strain field. In this section, to further carry out the distribution and gradient characteristics of internal stress caused by damages, the influence of cutting speed and depth on above features in feed direction were further calculated in Fig. 8.

Among all of cases, Fig. 8 (a-d) showed the influence of cutting speed on subsurface inner stress state when the cutting distance reached 20 μm. At low cutting speeds, subsurface defects have to suffer from more complicated and prolonged external stress state so that more of mobile dislocations were blocked by precipitates and obstacles in near-surface zone, which directly resulted in the severe stress concentration features in Fig. 8 (a-b). However, while the cutting speed increased in feed direction, the amplitude of subsurface inner stress σ_{11} decreased, reached minimum 160 MPa around 40 m/s, as shown in Fig. 8 (c-d). It is noted that although the phenomenon of internal stress polarization was significantly alleviated accompanying increase of cutting speed, the quantity of stress concentration regions (SCRs) also increased. The result agrees well with previous simulations, in fact, it can be explained that the motions of dislocations from local lattice to neighboring is more easily thwarted by refinement grain so that large amount of dislocations would be increasingly fragmented into different grains, which leads to the decrease of gradient magnitude of inner stress.

Fig. 8 (e-h) showed the evolution process of subsurface inner stress under various cutting depths when the cutting length is 5 μm. Through comparison among Figures, subsurface damages structure configurations evolved from simpleness to complexity and the inner stress was increasingly polarized with the increase of cutting depth. At the same time, rising energy aggregation facilitates dislocations nucleation and generates cross slip bands and straight slip bands span multiple grains. In Fig. 8 (e), sporadic SRCs were randomly distributed in near-surface

damage layer. As the axial depth of cut increased, a distinct distinction can be found that the distribution area of high stress σ_{11} gradually enlarged and the location of SRCs spilt over into subsurface internal region step by step in Fig. 8 (f-h). The essential factor is that the large axial depth of cut induces seriously shock wave into titanium alloy subsurface [38], which leads to the distortion of grain boundaries and the aberrance of lattice in deep-surface layer (in Fig. 8 (h)). With the increase of accumulative inhomogeneous, the crowding in or out in lattice boundaries may further exacerbate the phenomenon of inner stress concentration in surrounding lattices and result in intergranular fracture at internal deep-surface damage layer.

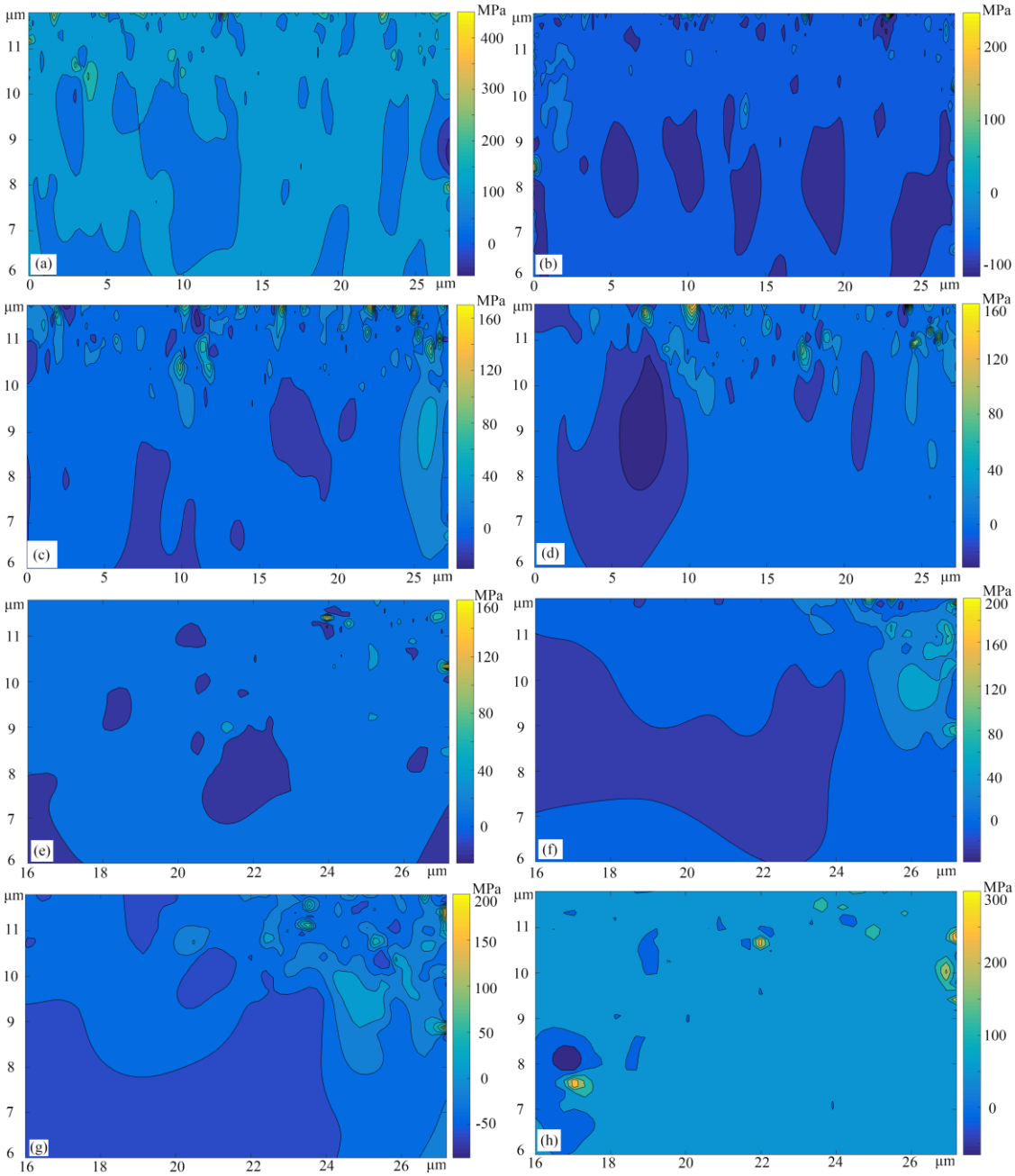

Fig. 8 Influence of cutting speed on subsurface inner stress distribution. (a) cutting speed 10 m/s; (b) cutting speed 20 m/s; (c) cutting speed 30 m/s; (d) cutting speed 40 m/s. (depth of cut = 1μm; cutting distance = 20 μm); Influence of axial depth of cut on subsurface inner stress state distribution. (e) cutting depth 0.5 μm; (f) cutting depth 1 μm; (g) cutting depth 2 μm; (h) cutting depth 3 μm. (cutting speed = 10m/s; cutting distance = 5 μm).

5 Conclusions

In this paper, a trans-scale simulation framework was presented to reveal detailed insight into the damage formation and propagation during micro-cutting titanium alloy process. The present study was particular concerned about the dependency between cutting parameters and subsurface defect structure. Following conclusions were obtained:

(a) A dislocation dynamics-based predictive model was performed to obtain the subsurface plastic deformation and microstructure alteration during processing. The novel FEM modeling technique embedded with discrete dislocation dynamics subroutine was given to reveal the interaction mechanism among dislocations and other defects. The predicted mechanism is identical with previous experimental findings on machined subsurface, which demonstrates the dislocation dynamics-based framework is a useful tool to quantitatively trace the microstructural evolution of subsurface defect.

(b) The prime formation mechanism of subsurface defect structure is dislocation motion and grain refinement. During steady micro-machining process, subsurface damage layer possesses a series of invariable characteristic such as, dislocation multiplication, slant dislocation lines, dense dislocation bands and dynamic recrystallization.

(c) Two different natures of subsurface damage layers are indicated, near-surface damage layer and deep-surface damage layer, respectively. Particularly, the emergence of near-surface damage layer is always accompanied with the appearance of subsurface work-hardening. Instead, the dislocation evolution in deep-surface deformation zone may produce the local strain softening phenomenon under certain processing conditions.

(d) The depth of subsurface damage layer generated in micro-cutting process is directly related to cutting depth and cutting speed. Increasing cutting depth induces subsurface damages as well as activates dislocation generation and movement deep in subsurface interior. Furthermore, large cutting speed would significantly boost the diffusion coefficient of dislocation, which can promote grain refinement and inhibit dislocation nucleation in deep-surface damage layer.

(e) The distribution of internal stress patterns and SCRs is severely influenced by processing parameters, which results in the distortion and aberrance of subsurface lattice. Moreover, it should be noted that the micro-crack may be nucleation not only in the near-surface hardening zone but also in the internal deep-surface damage layer.

Acknowledgments

This research work was jointly supported by the National Natural Science Foundation of China (Grant No. 51575138) and the State Key Program of National Natural Science Foundation of China (Grant No. 51535003).

References

[1]. L. Tan, D.H. Zhang, C.F. Yao, D.X. Wu, J.Y Zhang: Evolution and empirical modeling of compressive residual stress profile after milling, polishing and shot peening for TC17 alloy. J. Manuf. Process. 26, 155-165 (2017).

[2]. R.M. Saoubi, J.C. Outeiro, H. Chandrasekaran, O.W. Dillon, I.S. Jawahir: A review of surface integrity in machining and its impact on functional performance and life of machined products. Int. J. Sustain. Manufact. 1(1-2), 203–236 (2008).

[3]. D. Ulutan, T. Ozel: Machining induced surface integrity in titanium and nickel alloys: A review. Int. J. Mach. Tool. Manu. 51, 250-280 (2011).

[4]. T.H. Tan, J.W. Yan: Atomic-scale characterization of subsurface damage and structural changes of single-crystal silicon carbide subjected to electrical discharge machining. Acta. Mater. 123, 362-372 (2017).

[5]. C.H. Che-Haron: Tool life and surface integrity in turning titanium alloy. J. Mater. Process. Tech. 118, 231–237 (2001).

[6]. A.R.C. Sharman, J.J. Hughes, K. Ridgway: Workpiece surface integrity and tool life issues when turning Inconel 718 nickel based superalloy. Mach. Sci. Technol. 8(3), 399–414 (2004).

[7]. V. Bushlya, J.M. Zhou, J.E. Stahl: Modeling and experimentation on multistage work-hardening mechanism in machining with nose-radiused tools and its influence on machined subsurface quality and tool wear. Int. J. Adv. Manuf. Tech. 73, 545-555 (2014).

[8]. I.S. Jawahir, E. Brinksmeier, R.M. Saoubi, D.K. Aspinwall, J.C. Outeiro, D. Meyer, D. Umbrello, A.D. Jayal: Surface integrity in material removal processes: Recent advances. CIRP Ann-Manuf Techn. 60, 603-626 (2011).

[9]. A. Ginting, M. Nouari: Surface integrity of dry machined titanium alloys. Int. J. Mach. Tool. Manufact. 49(3–4), 325–332 (2009).

[10]. M. Thomas, S. Turnerb, M. Jackson: Microstructural damage during high-speed milling of titanium alloys. Scripta Mater. 62, 250-253 (2010).

[11]. J. Kwong. D. A. Axinte, P. J. Withers: The sensitivity of Ni-based superalloy to hole making operations: Influence of process parameters on subsurface damage and residual stress. J. Master. Process. Technol. 209(8), 3968-3977 (2009).

[12]. D. Jin, Z.Q. Liu: Damage of the machined surface and subsurface in orthogonal milling of FGH95 superalloy. Int. J. Adv. Manuf. Tech. 68, 1573-1581 (2013).

[13]. D.X. Lv, H.X. Wang, W.W. Zhang, Z.Q. Yin: Subsurface damage depth and distribution in rotary ultrasonic machining and conventional grinding of glass BK7. Int. J. Adv. Manuf. Tech. 86, 2361-2371 (2016).

[14]. S.J. Zhang, S. To, C.F. Cheung, Y. Zhu: Micro-structural changes of Zn-Al alloy influencing micro-topographical surface in micro-cutting. Int. J. Adv. Manuf. Tech. 72(1–4), 9–15 (2014).

[15]. J.X. Bai, Q.S. Bai, Z. Tong, C. Hu, X. He: Evolution of surface grain structure and mechanical properties in orthogonal cutting of titanium alloy. J. Mater. Res. 31(24), 1-11 (2016).

[16]. Y.B. Guo, W. Li, I.S. Jawahir: Surface integrity characterization and prediction in machining of hardened and difficult-to-machine alloys: a state-of-the-art research review and analysis. Mach. Sci. Technol. 13, 437–470 (2009).

[17]. M.M. Gurusamy, B.C. Rao: On the performance of modified Zerilli-Armstrong constitutive model in simulating the metal-cutting process. J. Manuf. Process. 28, 253-265 (2017).

[18]. H.T. Ding, Y.C. Shin: Multi-physics modeling and simulations of surface microstructure alteration in hard turning. J. Master. Process. Technol. 213, 877-886 (2013).

[19]. S. Hore, S.K. Das, S. Banerjee, S. Mukherjee: Computational modelling of static recrystallization and two dimensional microstructure evolution during hot strip rolling of advanced high strength steel. J. Master. Process. Technol. 17, 78-87 (2015).

[20]. Q.L. Wang, Q.S. Bai, J.X. Chen, Y.B. Guo, W.K. Xie: Stress-induced formation mechanism of stacking fault tetrahedra in nano-cutting of single crystal copper. Appl. Surf. Sci. 355, 1153-1160 (2015).

[21]. J. Li, Q.H. Fang, Y.W. Liu, L.C. Zhang: A molecular dynamics investigation into the mechanisms of subsurface damage and material removal of monocrystalline copper subjected to nanoscale high speed grinding. Appl. Surf. Sci. 303, 331-343 (2014).

[22]. S.S. Shishvan, E. Van der Giessen: Mode I crack analysis in single crystals with anisotropic discrete dislocation plasticity: I. Formation and crack growth. Modell. Simul. Mater. Sci. Eng. 21, 065006 (2013).

[23]. S.S. Shishvan, E. Van der Giessen: Mode I crack analysis in single crystals with anisotropic discrete dislocation plasticity: II. Stationary crack-tip fields. 21, 065007 (2013).

[24]. E. Tarleton, D.S. Balint, J. Gong, A.K. Wilkinson: A discrete dislocation plasticity study of the

micro-cantilever size effect. Acta. Mater. 88, 271–282 (2015).
[25]. C.H. Che-Haron, A. Jawaid: The effect of machining on surface integrity of titanium alloy Ti-6Al-4V. J. Mater. Process. Tech. 166, 188–192 (2005).
[26]. P. Crawforth, B. Wynne, S. Turnerb, M. Jackson: Subsurface deformation during precision turning of a near-alpha titanium alloy. Scripta. Mater. 67, 842–845 (2012).
[27]. M.J. Bermingham, S.D. McDonald, M.S. Dargusch, D.H. StJohn: Grain-refinement mechanisms in titanium alloys. J. Mater. Res. 23(1), 97-104 (2008).
[28]. Q.Q. Wang, Z.Q. Liu, B. Wang, Q.H. Song, Y. Wan: Evolutions of grain size and micro-hardness during chip formation and machined surface generation for Ti-6Al-4V in high-speed machining. Int. J. Adv. Manuf. Tech. 82, 1725-1736 (2016).
[29]. C.J. Ouyang, Z.H. Li, M.S. Huang, C.T. Hou: Discrete dislocation analyses of circular nanoindentation and its size dependence in polycrystals. Acta. Mater. 56, 2706–2717 (2008).
[30]. N. Ahmed, A. Hartmaier: A two-dimensional dislocation dynamics model of the plastic deformation of polycrystalline metals. J. Mech. Phys. Solids. 58(12), 2054–2064 (2010).
[31]. A.A. Benzerga, Y. Brechet, A. Needleman, E. Van der Giessen: Incorporating three-dimensional mechanisms into two-dimension dislocation dynamics. Modell. Simul. Mater. Sci. Eng. 12(3), 159–196 (2004).
[32]. K.M. Davoudi, L. Nicola, J.J. Vlassak: Dislocation climb in two-dimensional discrete dislocation dynamics. J. Appl. Phys. 111(10), 103522 (2012).
[33]. K. Danas, V.S. Deshpande: Plane-strain discrete dislocation plasticity with climb-assisted glide motion of dislocations. Modell. Simul. Mater. Sci. Eng. 21(4), 45008–45033 (2013).
[34]. Y.C. Zhang, T. Mabrouki, D. Nelias, Y. D. Gong: Chip formation in orthogonal cutting considering interface limiting shear stress and damage evolution based on fracture energy approach. Finite. Elem. Anal. Des. 47, 850-863 (2011).
[35]. M.S. Huang, Z.H. Li: Coupled DDD–FEM modeling on the mechanical behavior of microlayered metallic multilayer film at elevated temperature. J. Mech. Phys. Solids. 85, 74-97 (2015).
[36]. J. Sun, Y.B. Guo: A comprehensive experimental study on surface integrity by end milling Ti–6Al–4V. J. Master. Process. Technol. 209, 4036–4042 (2009).
[37]. D.H. Shin, I. Kim, J. Kim, Y.S. Kim, S.L. Semiatin: Microstructure development during equal-channel angular pressing of titanium. Acta. Mater. 51, 83-996 (2003).
[38]. B. Jiang, T.T. He, Y.P. Gu, Q.L, Wang, G.L. Cao: Method for recognizing wave dynamics damage in high-speed milling cutter. Int. J. Adv. Manuf. Tech. 1-12 (2017).